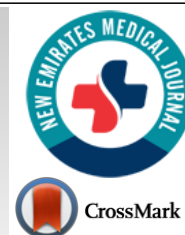




# New Emirates Medical Journal

Content list available at: <https://benthamscience.com/journal/nemj>



## RESEARCH ARTICLE

# Ligand-protein Docking of *Gundelia tournefortii* and *Ocimum basilicum* Derivatives in Scanning Hub Protein Targets (PI3K, PDK1, AKT, and RAC1) of the Insulin Signaling **Pathway and** ADME/Tox Drug Properties

Seema Tahayneh<sup>1</sup>, Baylasan Qasem<sup>1</sup>, Hadeel Zakarneh<sup>1</sup>, Siba Shanak<sup>1,\*</sup> and Hilal Zaid<sup>2,3</sup>

<sup>1</sup>Department of Biology and Biotechnology, Faculty of Sciences, Arab American University, P.O Box 240, Jenin, State of Palestine

<sup>2</sup>Department of Biochemistry, Faculty of Medicine, Arab American University, P.O Box 240, Jenin, State of Palestine

<sup>3</sup>Qasemi Research Center, Al-Qasemi Academic College, P.O Box 124, Baqa El-Gharbia 30100, Israel

### Abstract:

#### Background:

Type 2 diabetes is a heterogeneous disease characterized by high blood glucose levels. Its prevalence is increasing as a result of lifestyle, related genes expression, and insufficient insulin signaling. The activation or inhibition of some proteins in the insulin signaling pathway play a vital role in glucose uptake into the cells and in maintaining serum glucose homeostasis. Phosphoinositide-3-kinase (PI3K), 3-phosphoinositide-dependent protein kinase-1 (PDK1), Protein kinase B [PKB, also known as the serine and threonine kinase (AKT)], and Rac family small GTPase 1 (RAC1) are key proteins that play important roles in the liberation of Glucose Transported-4 (GLUT4) vesicle, and consequently the uptake of glucose in response to the insulin signal of hyperglycemia.

#### Objective:

In this study, we have focused on the route of targeting insulin signaling proteins for decreasing insulin resistance by targeting the four proteins, PI3K, PDK1, AKT, and RAC1, using *in silico* studies.

#### Methods:

Docking experiments, using AutoDock algorithms, were performed to predict the activity of eight recently purified derivatives of *Gundelia tournefortii* (GT) and *Ocimum basilicum* (4-hydroxybenzoic acid, beta-amyrin, beta-sitosterol, chlorogenic acid, lupeol, lupeol-trifluoroacetate, myo-inositol, and stigmasterol) on the insulin signaling proteins. The SwissADME website was used to predict ADMEtox properties for the eight derivatives of the above-mentioned medicinal plants.

#### Results:

Most of the *Gundelia tournefortii* and *Ocimum basilicum* derivatives have shown variable levels of activation, mainly on the PDK1 and AKT pathways, and to a much lesser extent on the PI3K and RAC1 pathways.

#### Conclusion:

The results have indicated that *Gundelia tournefortii* and *Ocimum basilicum* derivatives can be potent anti-diabetic drugs, namely in targeting PDK1 and AKT pathways.

**Keywords:** Diabetes mellitus, *Gundelia tournefortii*, *Ocimum basilicum*, Phytochemicals, *In silico*, Glucose level.

### Article History

Received: March 11, 2024

Revised: May 20, 2024

Accepted: May 27, 2024

## 1. INTRODUCTION

Diabetes mellitus is a group of metabolic illnesses with hyperglycemia being its common underlying feature [1]. The elevated glucose level is due to a deficiency in insulin secretion, insulin action, or most frequently both [2]. Diabetes

is widespread. The prevalence of DM increased from 108 million cases (4.7%) in 1980 to 425 million (8.5%) in 2017, and it is predicted to reach 629 million cases by 2045 [3]. The vast majority of diabetic patients fall into one of two broad categories. The first form is Type 1 Diabetes Mellitus (T1DM), which is an autoimmune condition that causes the death of pancreatic beta cells that produce insulin, leading to an absolute or near absolute deficiency of insulin [4, 5]. The latter

\* Address correspondence to this author at the Department of Biology and Biotechnology, Faculty of Sciences, Arab American University, P.O Box 240, Jenin, State of Palestine; E-mail: [siba.shanak@aaup.edu](mailto:siba.shanak@aaup.edu)

category is Type 2 Diabetes Mellitus (T2DM), which is characterized by the incidence of insulin resistance with an insufficient compensatory increase in insulin secretion [6]. A third less prevalent form of diabetes is Gestational Diabetes Mellitus (GDM). One in six live deliveries is complicated by GDM, which normally develops in the second or third trimesters of pregnancy [7]. Indeed, there are a variety of uncommon and diverse types of diabetes, which are caused by infections, drugs, endocrinopathies, pancreatic destruction, and genetic defects [2, 8 - 11]. Type 2 Diabetes Mellitus (T2DM) can be caused by flaws in one or more different molecular pathways due to its heterogeneity. It is frequently categorized as a monogenic disorder that primarily affects insulin action, either by involving molecules in the insulin signal transduction cascade or by causing abnormalities in the development of fat tissue (lipodystrophy), with secondary metabolic disturbances resulting in insulin resistance [6]. The human body controls the high level of glucose in the blood by several routes. One such route is the uptake of glucose by muscle and fat cells [12, 13]. This is achieved through the liberation of the intracellular Glucose Transporter 4 (GLUT4) and translocating it to the cellular membrane [14]. This action is a result of receiving the signal of insulin hormone in response to hyperglycemia [15]. Insulin binding to the insulin receptor stimulates several signaling cascades [16]. One cascade regulates gene expression and growth by means of a group of proteins, including SHC, Grb2, RAF, and MAP kinase known as the Ras/MAPK pathway [17]. Another cascade, on which our study has focused, is responsible for the translocation of GLUT4 vesicle to the cell membrane (Figs. 1 - 2) [18]. This pathway includes a set of activation and inhibition processes for a number of proteins, including IRS (Insulin Receptor Substrate), PI3K (Phosphoinositide-3-kinase), AS160 (Akt Substrate of 160 kDa), mTOR (mammalian Target of Rapamycin), etc [19]. The insulin pathway begins when insulin binds to an insulin receptor classified as tyrosine kinase. The binding process subsequently leads to the autophosphorylation and activation of tyrosine residues [20]. Phosphorylated tyrosine activates the IRS and a group of proteins as effectors to activate PI3K. PI3K consists of two basic units, regulatory (p85) and catalytic (p110 $\alpha$ ) subunits. The IRS-P85 binding induces p110 $\alpha$  to phosphorylate Phosphatidylinositol (4,5) bisphosphate (PI2P) and convert it to Phosphatidylinositol (3,4,5) trisphosphate (PI3P), located on the cell membrane [21]. 3-phosphoinositide-dependent protein Kinase-1 (PDK1) consists of two fundamental domains, PH domain and a kinase domain [22]. The kinase domain has three ligand binding sites, namely the substrate binding site, the ATP binding site, and the docking site also known as the PIF pocket. When the PH domain is activated by the PI3P, the kinase domain activates the AKT protein at THR308 [23]. Protein Kinase B (PKB) is also known as the serine and threonine kinase Akt. Three domains make up Akt: a specific PH domain, a central kinase domain, and a carboxyl-terminal regulatory domain [24]. The associated key actor in insulin signaling, Akt/PKB, acts from the cytosol directly to the plasma membrane. It binds precisely to a Pleckstrin Homology (PH) domain occurring at the Akt amino terminus, which is recruited as a result of the sustained increase in PIP3. Akt is phosphorylated particularly at THR308 and SER473 residues [25], which makes it act in a similar

fashion to Phosphoinositide-dependent Kinase-1 (PDK1) and mTOR Complex 2 (mTORC2). After becoming activated, AKT detaches from the plasma membrane and becomes heavily involved in the control of insulin-dependent activities, where it becomes phosphorylated by a variety of substrates [26]. Rac family small GTPase 1 (RAC1) has several domains, including the Nucleotide-binding Site (NBS), switches I and II, the multi-base region (PBR), and the CAAX box [27]. Switch II interacts with the RAC1 activation protein Guanine nucleotide Exchange Factor (GEF), while switch I primarily interacts with the downstream effectors of RAC1 [27].

As shown in Fig. (2) [28], insulin causes the PI3K-dependent activation of candidate Guanine nucleotide Exchange Factors (GEFs) or the deactivation of possible GTPase-activating Proteins (GAPs), which in turn causes Rac1 to load up on GTP. As a result of RAC1 activation, insulin-stimulated GLUT4 translocation follows [27, 29].

The recommended initial approach for the treatment of T2DM includes a combination of effective lifestyle changes and medication use [30 - 32]. Medications mainly focus on reducing insulin resistance and lowering the risk of macrovascular and microvascular complications [32 - 34]. This can be achieved by reaching near-normal glycated haemoglobin [35, 36]. Food and Drug Administration (FDA) has approved many antidiabetic drugs that produce clinical effects through different mechanisms. These medications include biguanides, such as metformin, which reduce gluconeogenesis in the liver [37]; insulin sensitizers, including thiazolidinediones, which improve insulin sensitivity in peripheral tissues [38]; insulin supplied in the form of recombinant insulin or analogues of it [39, 40]. Two medicinal plant species, *Gundelia tournefortii* L. and *Ocimum basilicum*, are commonly used to extract therapeutic phytochemicals and are common in the Middle East culture [41 - 44]. The artichoke-like vegetable *Gundelia tournefortii* L. thrives in the semi-arid environment of several Mediterranean nations [42]. Its common name is tumble thistle, and it is a member of the *Compositae* or *Asteraceae* families [45]. The plant is also known as *Tournefort's gundelia*. It is a spiky perennial, and the sections that are above the soil's surface have the potential to break, aiding the distribution of seeds. GT is a wild edible plant with antibacterial, anticancer, antiepileptic, anti-diabetic, and anti-epileptic properties [41, 42, 45]. *O. basilicum* has many therapeutic characteristics. It originated in the Asian continent and is now widely grown as an herbaceous perennial plant. *O. basilicum* belongs to *Lamiaceae* and possesses several pharmacological properties that can be used to prevent or cure cancer, diabetes, menstrual cramps, digestive issues, cardiovascular diseases, and other illnesses [44, 46, 47]. Additionally, it has been linked to reports of antioxidant, antibacterial, and larvicidal properties [48]. Obtaining a ligand-receptor complex with optimal shape complementarity and minimal binding free energy is the main goal of molecular docking [49]. The *in silico* ADME/Tox profile is a helpful tool for predicting the pharmacological and toxicological features of drug candidates, especially in the pre-clinical stages [50]. The use of *in silico* models has improved ADME/Tox predictions [51]. The use of these models is particularly helpful for drug optimization and preventing late-stage failures, which

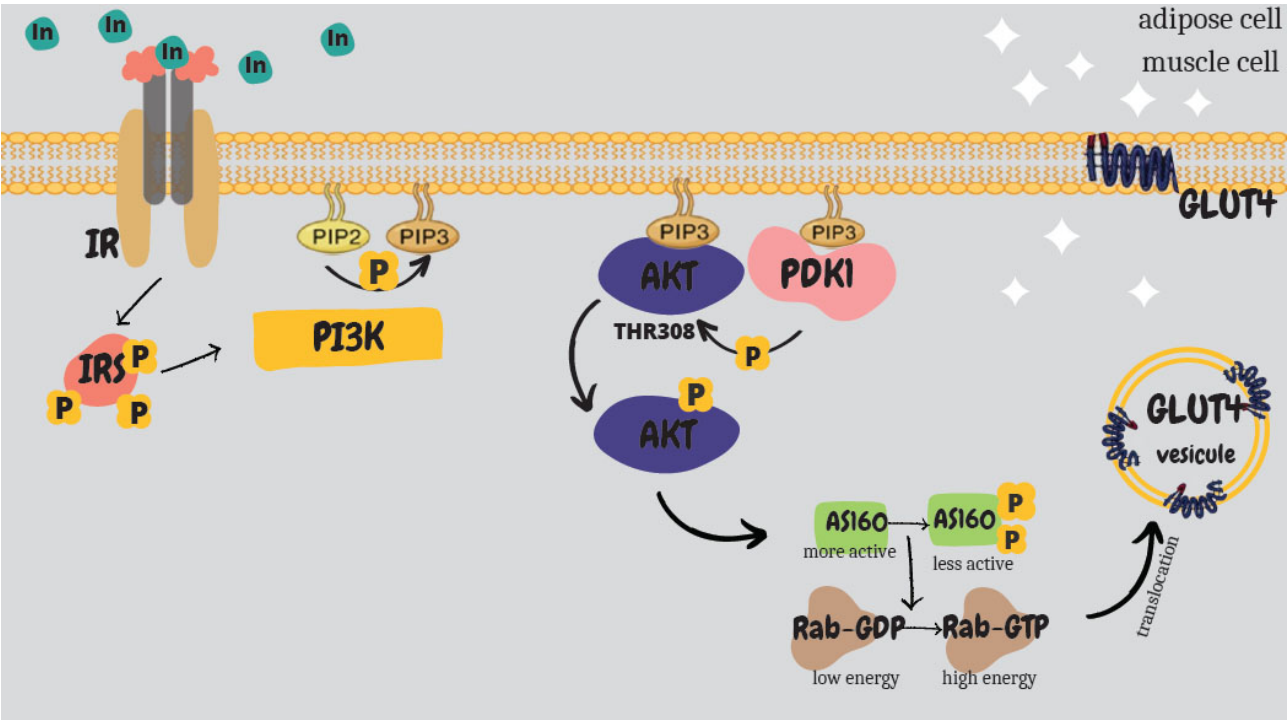


Fig. (1). PI3K/AKT insulin signaling pathway [26]. In this pathway, PI3K, PDK1, and AKT proteins are included.

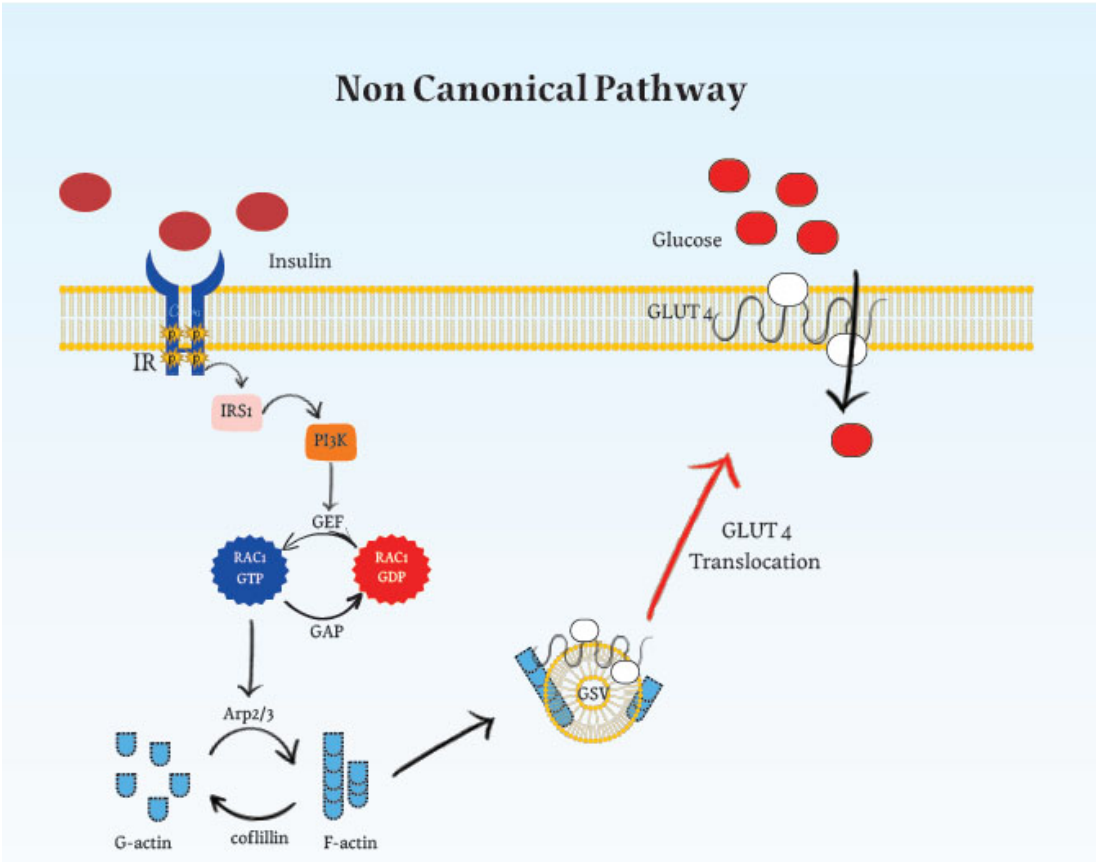


Fig. (2). Non-canonical insulin signaling pathway [28]. In this pathway, the RAC1 protein is included.

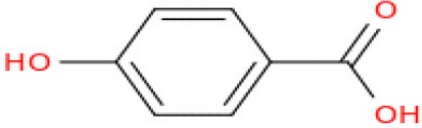
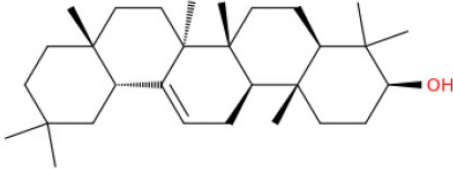
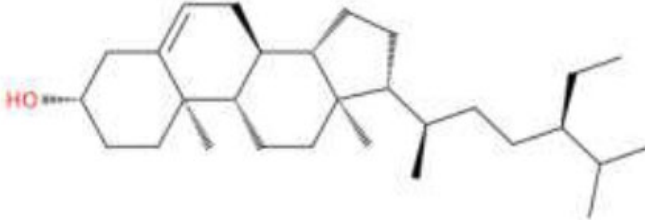
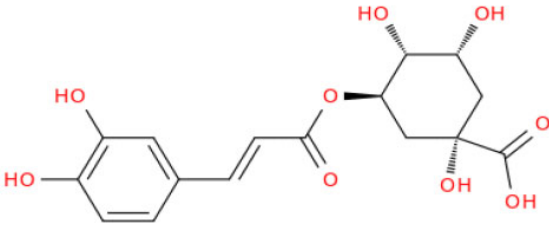
is crucial since late-stage failures result in a significant loss of time and money. The term ADME/Tox is used to explain how medications are absorbed, distributed, metabolized, and excreted, and the level of their toxicity [51, 52]. In this study, we aimed to predict the plausible efficiency of eight phytochemical extracts of the *Gundelia tournefortii* L. and *Ocimum basilicum* medicinal plants in targeting hub proteins (PDK1, PI3K, AKT, and RAC1) of the insulin signaling cascade, which affect the GLUT4 translocation to the plasma membrane. To this aim, docking and ADME/Tox algorithms have been used to achieve priori knowledge for further *in vitro*, *in vivo*, and clinical studies. We could predict that these phytochemicals work as agonists for PI3K, PDK1, AKT, and RAC1, and as a result, increase GLUT4 translocation to the plasma membrane.

## 2. MATERIALS AND METHODS


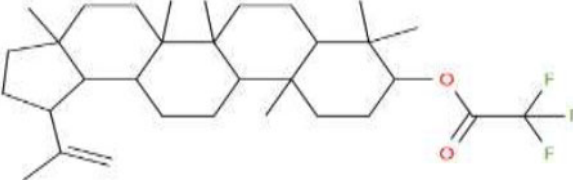
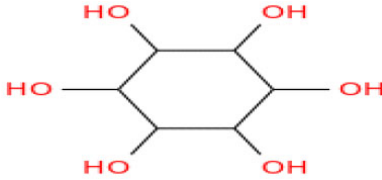
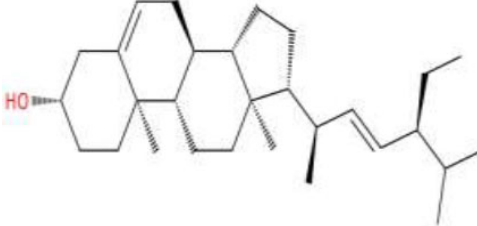
### 2.1. Docking Experiments Investigating *Gundelia Tournefortii*'s and *Ocimum Basilicum*'s Natural Effector Ligands that Bind to the Protein Targets of Insulin Signalling Pathway

The phytochemicals were extracted and purified previously by Kadan and colleagues [45, 53, 54]. We obtained the 2D structures and IUPAC names for *Gundelia tournefortii* and *Ocimum basilicum* derivatives using the PubChem database (Table 1) [55]. SMILES structures of the compounds were determined using the systematic IUPAC structures [56]. The Open Babel server was used to produce the PDB structures for the ligands used as inputs in the AutoDock tools version 1.5.7 [57, 58].

**Table 1. Phytochemical derivatives of *Gundelia tournefortii* and *Ocimum basilicum*.**

-	Name and Structure	Plant
(1) 4-hydroxybenzoic acid	 4-Hydroxybenzoic acid	<i>Gundelia tournefortii</i>
(2) Beta-amyrin	 (3 <i>S</i> ,4 <i>aR</i> ,6 <i>aR</i> ,6 <i>bS</i> ,8 <i>aR</i> ,12 <i>aR</i> ,14 <i>aR</i> ,14 <i>bR</i> ) -4,4,6 <i>a</i> ,6 <i>b</i> ,8 <i>a</i> ,11,11,14 <i>b</i> -octamethyl- 1,2,3,4 <i>a</i> ,5,6,7,8,9,10,12,12 <i>a</i> ,14, 14 <i>a</i> -tetradecahydricipen-3-ol	<i>Gundelia tournefortii</i>
(3) Beta-sitosterol	 (3 <i>S</i> ,8 <i>S</i> ,9 <i>S</i> ,10 <i>R</i> ,13 <i>R</i> ,14 <i>S</i> ,17 <i>R</i> ) -17-[(2 <i>R</i> ,5 <i>R</i> )-5-ethyl-6-methylheptan- 2-yl]-10,13-dimethyl- 2,3,4,7,8,9,11,12,14,15,16,17- dodecahydro-1 <i>H</i> -cyclopenta[ <i>a</i> ]phenanthren-3-ol	<i>Gundelia tournefortii</i> , <i>Ocimum basilicum</i>
(4) Chlorogenic acid	 (1 <i>S</i> ,3 <i>R</i> ,4 <i>R</i> ,5 <i>R</i> )-3-[( <i>E</i> )-3-(3,4-dihydroxyphenyl) prop-2-enoyl]oxy-1,4,5-trihydroxycyclohexane -1-carboxylic acid	<i>Gundelia tournefortii</i> , <i>Ocimum basilicum</i>

(Table 1) contd.....

-	Name and Structure	Plant
(5) Lupeol	 (1R,3aR,5aR,5bR,7aR,9S,11aR,11bR,13aR,13bR)-3a,5a,5b,8,8,11a-hexamethyl-1-prop-1-en-2-yl-1,2,3,4,5,6,7,7a,9,10,11,11b,12,13,13a,13b-hexadecahydrocyclopenta[a]chrysen-9-ol	<i>Gundelia tournefortii</i>
(6) Lupeol, trifluoroacetate	 (3a,5a,5b,8,8,11a-hexamethyl-1-prop-1-en-2-yl-1,2,3,4,5,6,7,7a,9,10,11,11b,12,13,13a,13b-hexadecahydrocyclopenta[a]chrysen-9-yl) 2,2,2-trifluoroacetate	<i>Gundelia tournefortii</i>
(7) Myo-inositol	 Cyclohexane-1,2,3,4,5,6-hexol	<i>Gundelia tournefortii</i>
(8) Stigmasterol	 (3S,8S,9S,10R,13R,14S,17R)-17-[(E,2R,5S)-5-ethyl-6-methylhept-3-en-2-yl]-10,13-dimethyl-2,3,4,7,8,9,11,12,14,15,16,17-dodecahydro-1H-cyclopenta[a]phenanthren-3-ol	<i>Gundelia tournefortii</i>

We used the RCSB database to extract the structures of the PI3K, PDK1, AKT, and RAC1 proteins in the *holo*- form, where the protein was bonded to a positive control (activator) (PDB ID: 6OAC [59], PDB ID: 3HRF [60], PDB ID: 2UVM [61], and PDB ID: 2FJU [26], respectively). Afterward, we removed the activator to convert the protein to the *apo*- form. These files were then prepared as input files for the docking protocol using the 4.2 version of the AutoDock software [62]. The genetic algorithm was used to prepare for a docking protocol with a rigid protein and a flexible ligand [63]. In preparing files for docking, some modifications were performed, such as adding polar hydrogen atoms and removing water. Afterward, a grid box was created, defining the surface region to be scanned by the ligand at the protein surface. Any region outside the box was not explored during docking. Two scenarios of docking were established. In the first scenario, docking covered and searched the entire protein surface for compatible binding. The dimensions for the grid boxes covering PI3K, PDK1, AKT, and RAC1 total surfaces were

126 x 126 x 126 Å, 126 x 126 x 126 Å, 126 x 86 x 108 Å, and 126 x 100 x 100 Å, respectively [64]. In the second scenario, the grid box covered the site where the positive control was bonded to the protein. We aimed to find suitable analogues for the positive controls. The dimensions for the grid boxes of PI3K, PDK1, AKT, and RAC1 were 10.23 x 10.375 x 8.946 Å, 9.52 x 6.172 x 6.23 Å, 14 x 10 x 16 Å, and 9 x 9.6 x 11 Å, respectively. Twenty independent docking runs were carried out for each mentioned scenario. Of the resulting PDB files, the files with the lowest free energies and inhibition constants were ranked first, and the results they contained were extracted. PyMol 2.3 software was then used for 3D visualization of the 'best fit' of the proteins and ligands [65].

## 2.2. Validation

The docking procedure was validated by removing the activator from the crystal structure (thus generating the protein *apo*- form), and re-docking the activator into the activator binding site, or alternatively to the entire surface of the protein.

To this aim, AutoDock 4.2 was used [66]. Validation helps in finding out whether, using AutoDock, the activator binds precisely to the active site cleft and exhibits minimal variation from the real 3D structure in the *holo*- form. PyMOL 2.3 was then used to superimpose the re-docked complex onto the reference 3D complex [67].

### 2.3. ADME/Tox Properties

Using the swissADME website [51], we studied the properties of each phytochemical, mainly water solubility, pharmacokinetics, and several other variables mentioned in Table 2 by using the SMILES formula [56].

## 3. RESULTS

### 3.1. ADME/Tox Properties

Studying the ADME/Tox properties mentioned in Table 2 below, the phytochemicals showed variable levels of druggability (Table 2). 4-hydroxybenzoic acid showed high gastrointestinal tract absorption. Most phytochemicals obeyed Lipinski's rule of five, except for lupeol-trifluoroacetate. LogP

value should be positive in value and ideally <5 [68]. This way, a drug has a balanced hydrophobic index that allows it to pass membranes as well as be dissolved in aqueous environments. Again, 4-hydroxybenzoic acid optimally follows this rule. Most drugs showed robust scores for bioavailability ( $\geq 0.55$  [69]), except for chlorogenic acid and lupeol-trifluoroacetate. The six cytochrome P450 enzymes responsible for metabolizing 90% of the drugs in the body [70] were found to be not inhibited by most of the phytochemicals. Most drugs could not pass the blood-brain barrier, except for 4-hydroxybenzoic acid and lupeol-trifluoroacetate.

### 3.2. Binding-free Energies and Inhibition Constants for PI3K, PDK1, AKT, and RAC1

*Gundelia tournefortii* and *Ocimum basilicum* derivatives were tested for their binding affinities, inhibition constants, and Root Mean Square Deviation (RMSD) values for the ligand structure upon docking from the reference structure. Docking experiments showed variable binding strengths for the different phytochemicals. All results shown below have been obtained upon scanning the whole protein surface by several phytochemicals.

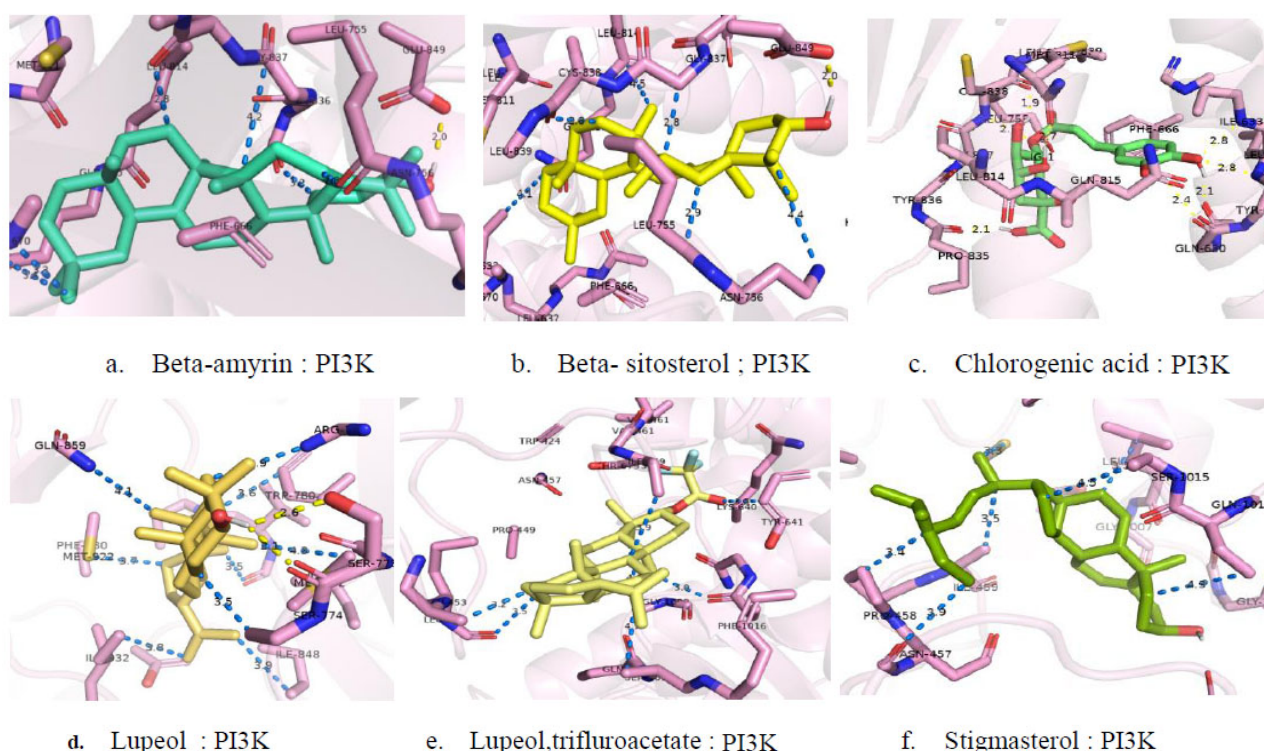
**Table 2. ADME/Tox properties of the *Gundelia tournefortii* and *Ocimum basilicum* derivatives.**

Phytochemicals	4-hydroxybenzoic Acid	Beta-amyrin	Beta-sitosterol	Chlorogenic Acid	Lupeol	Lupeol, Trifluoroacetate	Myo-inositol	Stigmasterol
GI absorption	High	Low	Low	Low	Low	Low	Low	Low
Lipinski	Yes; 0 violation	Yes; 1 violation: MLOG P>4.15	Yes; 1 violation: MLOG P>4.15	Yes; 1 violation: NH <sub>2</sub> OH>5	Yes; 1 violation: MLOG P>4.15	No violation: MW>500, MLOG P>4.15	Yes; 1 violation: MLOG P>4.15	Yes; 1 violation: MLOG P>4.15
Bioavailability	0.85	0.55	0.55	0.11	0.55	0.17	0.55	0.55
Log $p_{a/w}$	1.05	7.16	7.24	-0.39	7.27	8.43	-2.67	6.98
CYP1A2 inhibitor	No	No	No	No	No	No	No	No
CYP2CAP inhibitor	No	No	No	No	No	No	No	No
CYP2C9 inhibitor	No	No	No	No	No	No	No	Yes
CYP2D6 inhibitor	No	No	No	No	No	No	No	No
CYP3A4 inhibitor	No	No	No	No	No	No	No	No
BBB permeation	Yes	No	No	No	No	Yes	No	Yes

**Table 3. Activation action for the eight selected phytochemicals against the PI3K. Results that were considered as 'robust' are shaded in purple.**

Protein	Activator	AutoDock Binding Free Energy (Kcal/mol)	AutoDock Inhibition Constant, Ki	RMSD for the Ligand from the Reference Structure (Å)	No. of Polar Contacts	Amino Acids Involved in the Polar Interaction
PI3K (PDB ID: 6OAC 59)	4-hydroxybenzoic acid	-4.19	847.29μM	14.882	-	-
	Beta-amyrin	-11.22	5.99nm	26.472	1	GLU849
	Beta-sitosterol	-11.21	6.05nm	26.402	1	GLU849
	Chlorogenic acid	-5.05	198.61μM	26.321	8	MET811, PRO835, CYS838(2), SER629, GLN630, LEU632, ILE633
	Lupeol	-9.76	70.09 nM	39.596	2	SER7732(2)
	Lupeol, trifluoroacetate	-9.85	60.52nM	11.972	0	-
	Myoinositol	-3.72	1.87mM	25.773	-	-
	Stigmasterol	-8.32	797.14nM	8.816	0	-





**Fig. (3a-f).** Binding interfaces of the most robust binding interfaces of six mentioned phytochemicals to the PI3K (PDB ID: 6OAC 59). Polar contacts are coloured yellow and nonpolar contacts are coloured blue. Amino acids in the range of 5 Å from the ligands are shown.

### 3.2.1. PI3K Docking

Docking experiments showed good activation results for six phytochemicals (beta-amyrin, beta-sitosterol, chlorogenic acid, lupeol, lupeol-trifluoroacetate, and stigmasterol). Binding free energies of the PI3K to the tested phytochemicals were in the range of -11.22 to -5.05 Kcal/mol, indicating strong contacts. As for the Ki values, they were divided into a low range (5.99nM to 797.14nM), indicating a strong activation, and a moderate value (198.61 µM for chlorogenic acid), considered acceptable (Table 3).

### 3.2.2. Binding Interface for PI3K

For the PI3K (PDB ID: 6OAC [59]), and in all the above-mentioned six ligand-protein interfaces, short-ranged (1.9-2.4 Å) and moderate length-ranged (2.5-2.8 Å) electrostatic interactions at the ligand-protein interface were present (Fig. 3). Longer bonds (more than 2.8 Å) also existed at the binding interface. The binding interfaces were influenced by a number of nonpolar amino acids (*e.g.*, ILE and MET in chlorogenic acid), which contributed to the polar contacts *via* the backbone atoms. Moreover, at the binding interfaces, both polar and charged amino acids had a significant role (*e.g.*, GLU in beta-amyrin and beta-sitosterol; SER in lupeol; and CYS, SER, and GLN in chlorogenic acid) (Fig. 3).

### 3.2.3. PDK1 Docking

Docking experiments showed good binding results, excluding D-pinitol, myoinositol, palmitic acid, and linalool

phytochemicals. Binding free energies of the PDK1 to the several phytochemicals were in the range of -8.81 - -4.51 kcal/mol, indicating strong contacts. The Ki values were divided into a low range (349.06nM-1.85µM), indicating a strong activation, and moderate slightly strong contacts within the range 63.22µM -107.63 µM (Table 4).

### 3.2.4. Binding Interface for PDK1

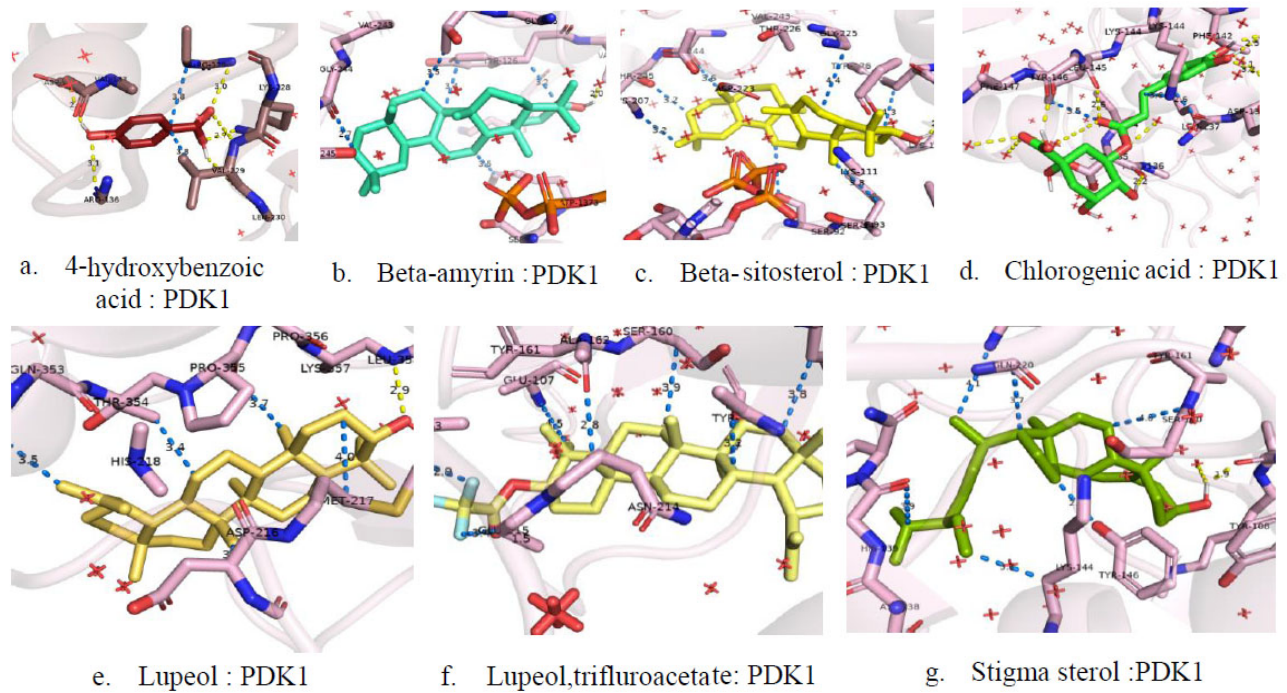
For the PDK1 (PDB ID: 3HRF [60]), and in six ligand-protein interaction interfaces, interactions at the ligand-protein interfaces were short-ranged (1.8 to 2.4 Å) and moderate-ranged (2.5 – 4.3 Å) electrostatic interactions (Fig. 4). The six ligands (phytochemicals) were 4-hydroxybenzoic acid, beta-amyrin, beta-sitosterol, chlorogenic acid, lupeol, and stigmasterol. Long-ranged interactions also existed at the binding interface. A number of nonpolar amino acids (*e.g.*, Tyr and Phe) contributed to the binding process. Moreover, at the binding interfaces, both polar and charged amino acids had a significant role (*e.g.*, Thr, Arg, and Lys).

### 3.2.5. AKT Docking

Docking experiments showed good activation results for eight phytochemicals. Binding free energies of the AKT to the several phytochemicals were in the range of -8.36 to -5.14Kcal/mol and indicated stable contacts. The Ki values of the AKT-binding interface to the tested phytochemicals were in a variable range (743.30 nM to 169.46 µM), indicating a strong activation (Table 5).

**Table 4.** Activation action of *Gundelia tournefortii* and *Ocimum basilicum* derivatives and eight selected phytochemicals against the PDK1. Results that were considered as ‘robust’ are shaded in purple.

Protein	Activator	AutoDock Binding Free Energy (Kcal/mol)	AutoDock Inhibition Constant, Ki	RMSD for the Ligand from the Reference Structure (Å)	No. of Polar Contacts (Only Significant Binding Results shown)	Amino Acids Involved in the Polar Interaction
PDK1 (PDB ID: 3HRF 60)	4-hydroxybenzoic acid	-5.56	84.63µM	30.681	4	ARG136, ASP132, VAL229, ARG129, LYS228
	Beta-amyrin	-8.43	662.66nM	32.588	0	VAL127
	Beta-sitosterol	-8.50	587.54nM	32.717	1	LYS123
	Chlorogenic acid	-5.41	107.63µM	25.332	6	SER135, HIS139, LUS145, TYR146(3)
	Lupeol	-7.82	1.85µM	44.670	1	LEU358
	Lupeol-trifluoroacetate	-8.81	349.06nM	35.507	0	-
	Myo-inositol	-3.85	1.51mM	35.088	-	-
	Stigmasterol	-7.79	1.94µM	36.862	1	GLU107



**Fig. (4).** Binding interfaces of the most robust binding interfaces of *Gundelia tournefortii* and *Ocimum basilicum* derivatives to the PDK1(PDB ID: 3HRF 60). Polar contacts are colored yellow and nonpolar contacts are colored blue. Amino acids in the range of 5 Å from the ligands are shown.

3.2.6. Binding Interface for AKT

For the AKT (PDB ID: 2UVM [61]), and in four ligand-protein interaction interfaces, short-ranged interactions (1 to 2.4 Å) were demonstrated. The four active phytochemicals were 4-hydroxybenzoic acid, chlorogenic acid, lupeol, and lupeol-trifluoroacetate. Moderate-ranged (2.5 to 3.5 Å) electrostatic interactions had higher contributions than the long-ranged (3.6 to 4.0 Å) interactions at the ligand-protein interface in the binding energies of the seven phytochemicals that showed good binding energies and Ki constants (Fig. 5). The binding interfaces were influenced by a number of nonpolar amino acids (e.g., ILE and VAL). Moreover, at the

binding interfaces, both polar and charged amino acids had a significant role (e.g., ARG, LYS, and THR).

3.2.7. RAC1 Docking Binding Free Energies and Inhibition Constants for the RAC1 Protein

Derivatives of *Gundelia tournefortii* and *Ocimum basilicum* were tested for their binding affinities, inhibition constants, and Root Mean Square Deviation (RMSD) values for the ligand structure upon docking from the reference structure. Docking of five phytochemicals (beta-amyrin, beta-sitosterol, lupeol, lupeol-trifluoroacetate, and stigmasterol) produced robust results in terms of binding free energies



Table 5. Activation action of eight selected phytochemical derivatives against the AKT. Results that were considered as ‘robust’ are shaded in purple.

Protein	Activator	AutoDock Binding Free Energy (Kcal/mol)	AutoDock Inhibition Constant, Ki	RMSD for the Ligand from the Reference Structure (Å)	No. of Polar Contacts	Amino Acids Involved in the Interaction
AKT (PDB ID: 2UVM 61)	4-hydroxybenzoic acid	-5.56	78.23µM	24.917	3	LYS-14, THR-87, ARG-15
	Beta amyrin	-8.36	743.30nm	9.807	0	-
	Beta sitosterol	-8.36	744.68nm	9.810	0	-
	Chlorogenic acid	-5.14	169.46µM	25.562	7	ARG-15(2), THR-87, ARG86(2), TYR18(2)
	Lupeol	-8.07	1.22 µM	23.126	1	VAL-83
	Lupeol, trifluoroacetate	-7.70	2.26µM	11.515	1	ASN-54
	Myoinositol	-4.21	817.95µM	7.609	-	-
	Stigmasterol	-7.37	3.97µM	15.615	0	-

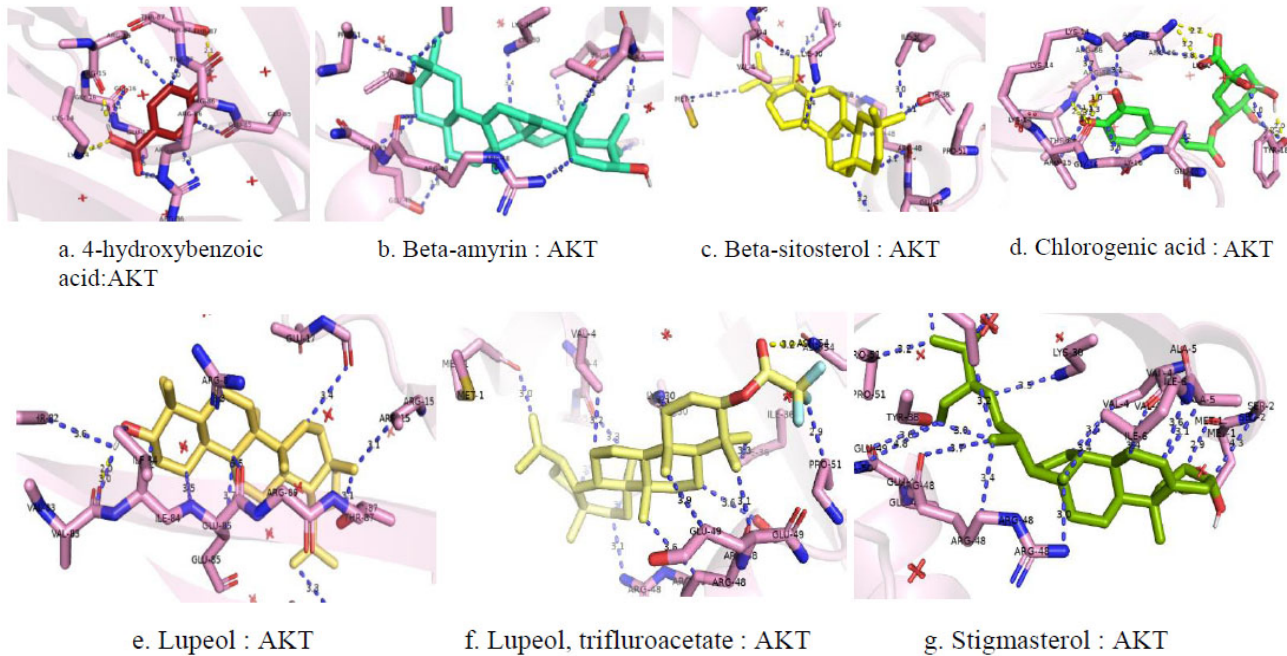
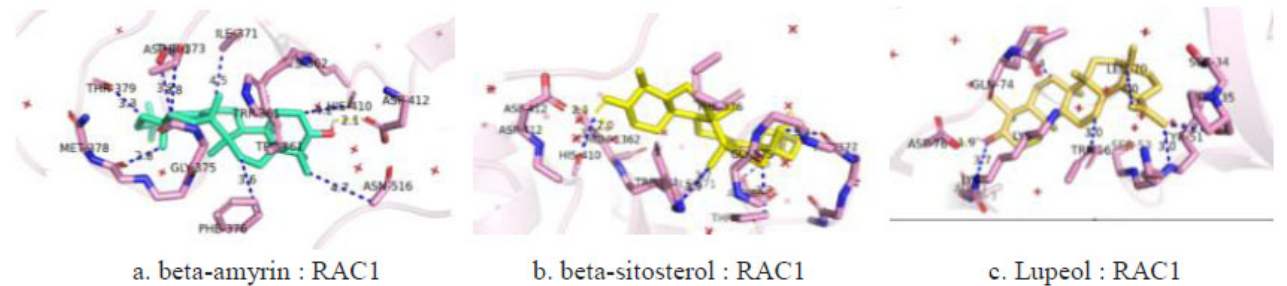
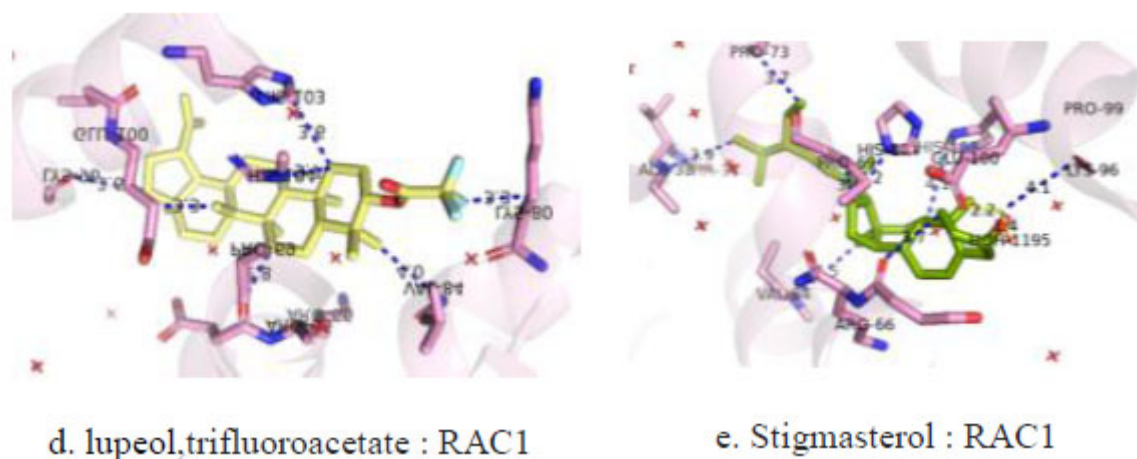


Fig. (5a-g). Binding interfaces of the most robust binding interfaces of most active phytochemicals to the AKT (PDB ID: 2UVM61). Polar contacts are coloured yellow and nonpolar contacts are coloured blue. Amino acids in the range of 5 Å from the ligands are shown.





**Fig. (6a-e).** Binding interfaces of five active phytochemicals to the RAC1 protein (PDB ID: 2FJU 26). Polar contacts are colored yellow and nonpolar contacts are colored blue.

**Table 6. Plausible protein activators of the eight selected phytochemicals for the RAC1 protein.**

Protein	Activator	AutoDock Binding Free Energy (Kcal/mol)	AutoDock Inhibition Constant, Ki	RMSD of the Ligand from the Reference Structure (Å)	No. of Polar Contacts	Amino Acids Involved in the Interactions
RAC1 (PDB ID: 2FJU 26)	4-hydroxybenzoic acid	-4.87	269.20 $\mu$ M	121.398	-	-
	Beta-amyrin	-8.78	365.08 nM	99.048	-	-
	Beta-sitosterol	-8.85	325.88 nM	98.915	1	ASP412
	Chlorogenic acid	-3.84	1.53 mM	93.946	-	-
	Lupeol	-8.63	472.41 nM	96.543	1	ASP67
	Lupeol-trifluoroacetate	-8.00	1.36 $\mu$ M	97.639	-	-
	Myo-inositol	-2.47	15.54 mM	126.190	-	-
	Stigmasterol	-7.16	5.61 $\mu$ M	96.265	-	GLU100

(ranging from -8.85 to -7.16 kcal/mol) and affinity constants (ranging from 472.41 nM to 5.61  $\mu$ M). Resultant bond lengths at the binding interfaces were classified into long-ranged (3.6 to 4.0 Å), moderate-ranged (2.5 to 3.5 Å), and short-ranged (1.4 to 2.4 Å) electrostatic interactions between the ligand and the protein (Fig. 6). Short-ranged interactions were found to affect the binding interfaces of beta-sitosterol, lupeol, and stigmasterol phytochemicals to the target RAC1 protein. Few longer bonds contributed to the binding process at the binding interface. The binding interfaces in the several binding schemes were influenced by a number of nonpolar amino acids (e.g., TRP, GLN, LYS, PHE, and THR). Moreover, at the binding interfaces, both polar and charged amino acids had significant contributions (e.g., ARG, PRO, ASP, GLU, and HIS) (Table 6).

### 3.3. Validation

Validation was conducted at the whole protein surface as well as at the binding interface. The validation results for the PDK1 and AKT on the whole protein surface were more significant than testing the binding of the positive control to its original binding site at the protein surface. In scanning the whole protein surface, very similar results to the original structure were achieved. The bonds were nearly the same as in

the main 3D structure, with a slight increase in around two bonds at the binding interfaces. In scanning the region where the positive ligand bonded to the original structure, variations were evident, as indicated in the tables and figures below. Validation results for binding of the positive control to the RAC1 and PI3K did not show good results. Results for validation at the whole binding interface as well as at the original binding sites are shown below in Tables 7 - 9 and Figs. (7 and 8). Figures have been only produced for the proteins that showed high binding affinities in scanning the whole protein surface and, at the same time, could bind close to the binding interface of the positive control. In scanning the whole surface, both crystal structures for the apo- and holo- forms of the proteins were used.

## 4. DISCUSSION

Phytochemicals and medicinal plant extracts have become major factors in drug development programs, especially because of minimal costs and fewer adverse effects [71, 72]. Indeed, the use of natural anti-diabetic drugs results in fewer side effects and is usually effective [73]. Recently, *Gundelia tournefortii* [45] and *Ocimum basilicum* [74] methanol extracts have been reported to efficiently augment GLUT4 translocation to the plasma membrane of skeletal muscle cells.

**Table 7. Validation of ligand binding to PI3K at the binding interface of the positive control and on the whole protein surface using the positive control extracted from the crystal structure.**

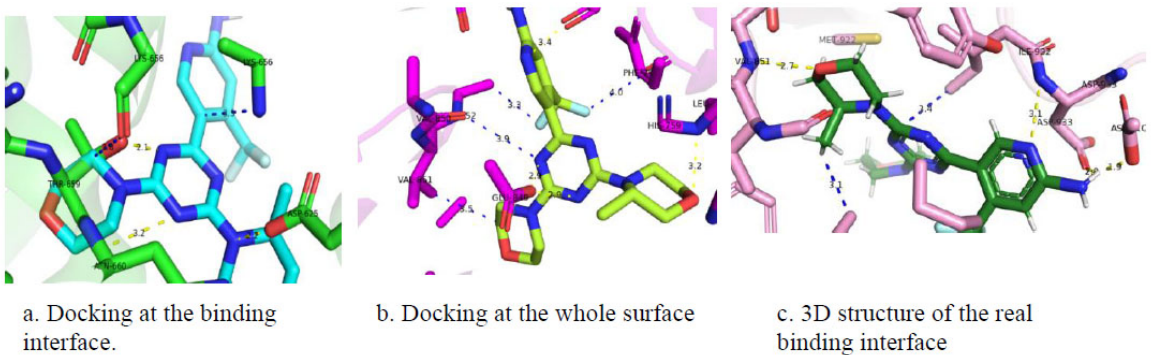
-	RMSD (Å)	Constant Activator (K <sub>i</sub> )	Binding Free Energy (kcal/mol)	No. of Hydrogen Bonds	Amino Acids Involved in Polar Contacts
Docking at the binding interface (PI3K, in the <i>apo</i> - form)	32.894	-	+4.46e+05	3	1(ASP625),2(THR659)
Docking at the whole surface (PI3K, in the <i>apo</i> - form)	40.565	990.95 nM	-8.19	1	1(HIS759)
PI3K (PDB ID: 6OAC 59) in the <i>holo</i> - form	-	-	-	3	2(ASP933), 1(VAL851)

**Table 8. Validation of ligand binding to PDK1 at the binding interface of the positive control and in scanning the whole surface, using the positive control that was extracted from the crystal structure.**

-	RMSD (Å)	Constant (K <sub>i</sub> ) “Activation”	Binding Free Energy kcal/mol	No. of Hydrogen Bonds	Amino Acids Involved in Polar Contacts
Docking at the binding interface (PDK1; in the <i>apo</i> - form.)	3.772	-	+8.59e+04	-	-
Docking at the whole surface (PDK1 in the <i>apo</i> - form)	2.218	1.22 μM	-8.07	3	1 (ARG-131), 2 (THR148)
PDK1 (PDB ID: 3HRF; 60) in the <i>holo</i> -form.	-	-	-	3	1(LYS76), 1(THR148), 1(ARG131)

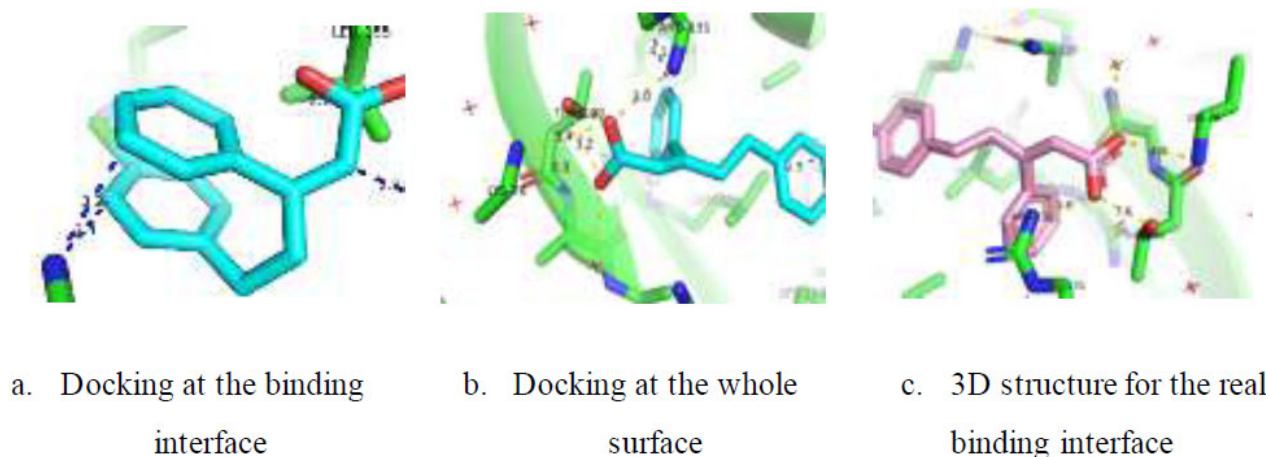
**Table 9. Validation of ligand binding to AKT at the binding interface of the positive control and in scanning the whole surface using the positive control, which was extracted from the crystal structure.**

-	RMSD (Å)	Constant Activator (K <sub>i</sub> )	Binding Free Energy, kcal/mol	No. of Hydrogen Bonds	Amino Acids Involved in Hydrogen Bonding
Docking at the binding interface (AKT, in the <i>apo</i> - form)	2.218	-	+1.89e+05	10	1 (LEU-52), 1 (ASN-53), 3 (LYN-14), 3 (ARG-23), 1 (ARG-15), 1 (GLU-17)
Docking at the whole surface (AKT; in the <i>apo</i> - form.)	1.860	757.57 nM	-8.35	18	6 (ARG-23), 2 (ARG-25), 1(ARG-86), 2(ASN-53), 4(LYN-14), 1(GLU-17), 1(TYR-18), 1(ILE-19)
AKT (PDB ID: 2UVM 61) in the <i>holo</i> -form.	-	-	-	16	5(ARG-23), 1(ARG-25), 2(ARG-86), 2(ASN-53), 2(LYN-14), 2(GLU-17), 1(TYR-18), 1(ILE-19)



**Fig. (7a-c).** Binding interfaces for the positive control to the PI3K (PDB ID: 6OAC 59) in the validation step. Polar contacts are coloured yellow and nonpolar contacts are coloured blue.





**Fig. (8a-c).** Binding interfaces for the positive control to the PDK1 (PDB ID: 3HRF 60) in the validation step . Polar contacts are coloured yellow and nonpolar contacts are coloured blue.

Ten phytochemicals have been detected in these herbal extracts. Among them, 8 have been reported to possess anti-diabetic activity and enhanced GLUT4 translocation to the PM, a main process in glucose disposal and homeostasis [75]. The phytochemicals have been investigated in this study. The mechanism of action on the insulin signalling pathway has not yet been investigated for *Gundelia tournefortii* and *Ocimum basilicum* derivatives. In our study, four hub proteins for insulin signalling pathway were tested for their plausible response to eight selected phytochemicals detected in the above-mentioned medicinal plants that are suggested to augment GLUT4 translocation to the plasma membrane, and thus enhance glucose disposal from the serum [45, 53, 54], with the consequent effect on GLUT4 translocation, alleviating hyperglycemia. We predicted the complementarity between the medical compounds and the target proteins by scoring schemes (RMSD, free energy, and inhibition constant). AKT and PDK1 were found here to be activated by all phytochemicals, except for myo-inositol, which had the lowest activation effect. On the other hand, RAC1 and PI3K showed good interaction results with some phytochemicals (beta-amyrin, beta-sitosterol, lupeol, lupeol-trifluoroacetate, and stigmasterol). PI3K could also be activated by chlorogenic acid. The binding free energies of the four proteins were slightly different. However, the RMSD values of the PDK1 and AKT proteins were closer to one another when compared to the PI3K and RAC1. However, in all proteins, myo-inositol showed the least activation action (with the highest inhibition constants and binding free energies) among all tested derivatives. In contrast, beta-amyrin, beta-sitosterol, lupeol, lupeol-trifluoroacetate, and stigmasterol showed positive results for PDK1, PI3K, AKT, and RAC1 proteins. By testing ADME/Tox features and reflecting our results with these characteristics, we deduced that several phytochemicals very well matched most of the ADME/Tox properties and are good candidates for oral administration. By using a validation step, we ensured the accuracy of the docking protocol by comparing the crystal structure, which is the actual association of the protein with its positive control, with the simulation of the association process through the docking process. The results for both PDK1 and AKT were very close

to the positive control binding to the reference structure. This was in contrast to PI3K and RAC1, for which the validation showed weak results compared to other proteins. We additionally predict that PI3K and RAC1 could not be plausible targets for the treatment of T2DM.

## CONCLUSION

Certain natural compounds may interact with protein hubs in insulin signalling, according to previous studies [26]. This study has highlighted the importance of these lead compounds in activating the AKT, PI3K, PDK1, and RAC1 proteins, which are hot topics for the catastrophic T2DM pandemic. Drug developers can assess the safety and effectiveness of a drug candidate using ADME/Tox features. We have found PDK1 and AKT to be more attractive protein targets for the studied lead compounds than the other proteins based on binding affinities, inhibition constants, binding interfaces, and ADME/Tox properties. These *in silico* outcomes offer strong bases for future *in vitro* and *in vivo* research and the discovery of possible medications to treat type II diabetes treatment. We believe that our study will motivate more work in this area.

## AUTHORS' CONTRIBUTION

It is hereby acknowledged that all authors have accepted responsibility for the manuscript's content and consented to its submission. They have meticulously reviewed all results and unanimously approved the final version of the manuscript.

## LIST OF ABBREVIATIONS

<b>PDK1</b>	=	Protein kinase-1
<b>AKT</b>	=	Threonine kinase
<b>RAC1</b>	=	Rac family small GTPase 1
<b>GLUT4</b>	=	Glucose Transported-4

## ETHICS APPROVAL AND CONSENT TO PARTICIPATE

Not applicable.



**HUMAN AND ANIMAL RIGHTS**

Not applicable.

**CONSENT FOR PUBLICATION**

Not applicable.

**AVAILABILITY OF DATA AND MATERIALS**

The data and supportive information are available within the article.

**FUNDING**

None.

**CONFLICT OF INTEREST**

The authors declare no conflict of interest, financial or otherwise.

**ACKNOWLEDGEMENTS**

The authors would like to thank the Arab American University/Palestine (AAUP) research foundation for supporting this study.

**REFERENCES**

- [1] Olaogun I, Farag M, Hamid P. The pathophysiology of type 2 diabetes mellitus in non-obese individuals: An overview of the current understanding. *Cureus* 2020; 12(4): e7614. [http://dx.doi.org/10.7759/cureus.7614] [PMID: 32399348]
- [2] Harreiter J, Roden M. Diabetes mellitus—definition, classification, diagnosis, screening and prevention (Update 2019). *Wien Klin Wochenschr* 2019; 131(S1)(Suppl. 1): 6-15. [http://dx.doi.org/10.1007/s00508-019-1450-4] [PMID: 30980151]
- [3] Glovaci D, Fan W, Wong ND. Epidemiology of diabetes mellitus and cardiovascular disease. *Curr Cardiol Rep* 2019; 21(4): 21. [http://dx.doi.org/10.1007/s11886-019-1107-y] [PMID: 30828746]
- [4] DiMeglio LA, Evans-Molina C, Oram RA. Type 1 diabetes. *Lancet* 2018; 391(10138): 2449-62. [http://dx.doi.org/10.1016/S0140-6736(18)31320-5] [PMID: 29916386]
- [5] Popoviciu MS, Kaka N, Sethi Y, Patel N, Chopra H, Cavalu S. Type 1 diabetes mellitus and autoimmune diseases: A critical review of the association and the application of personalized medicine. *J Pers Med* 2023; 13(3): 422. [http://dx.doi.org/10.3390/jpm13030422] [PMID: 36983604]
- [6] O'Rahilly S, Barroso I, Wareham NJ. Genetic factors in type 2 diabetes: The end of the beginning? *Science* 2005; 307(5708): 370-3. [http://dx.doi.org/10.1126/science.1104346] [PMID: 15662000]
- [7] Selen DJ, Powe CE. Gestational diabetes and other adverse pregnancy outcomes in polycystic ovary syndrome. *Curr Opin Endocrinol Diabetes Obes* 2022; 29(6): 521-7. [http://dx.doi.org/10.1097/MED.0000000000000769] [PMID: 35983844]
- [8] Kim EJ, Ha KH, Kim DJ, Choi YH. Diabetes and the risk of infection: A national cohort study. *Diabetes Metab J* 2019; 43(6): 804-14. [http://dx.doi.org/10.4093/dmj.2019.0071] [PMID: 31701687]
- [9] Pastor A, Conn J, MacIsaac RJ, Bonomo Y. Alcohol and illicit drug use in people with diabetes. *Lancet Diabetes Endocrinol* 2020; 8(3): 239-48. [http://dx.doi.org/10.1016/S2213-8587(19)30410-3] [PMID: 31958403]
- [10] Resmini E, Minuto F, Colao A, Ferone D. Secondary diabetes associated with principal endocrinopathies: The impact of new treatment modalities. *Acta Diabetol* 2009; 46(2): 85-95. [http://dx.doi.org/10.1007/s00592-009-0112-9] [PMID: 19322513]
- [11] Śliwińska-Mossoń M, Bil-Lula I, Marek G. The cause and effect relationship of diabetes after acute pancreatitis. *Biomedicines* 2023; 11(3): 667. [http://dx.doi.org/10.3390/biomedicines11030667] [PMID: 36979645]
- [12] Evans PL, McMillin SL, Weyrauch LA, Witczak CA. Regulation of skeletal muscle glucose transport and glucose metabolism by exercise training. *Nutrients* 2019; 11(10): 2432. [http://dx.doi.org/10.3390/nu11102432] [PMID: 31614762]
- [13] Chait A, den Hartigh LJ. Adipose tissue distribution, inflammation and its metabolic consequences, including diabetes and cardiovascular disease. *Front Cardiovasc Med* 2020; 7: 22. [http://dx.doi.org/10.3389/fcvm.2020.00022] [PMID: 32158768]
- [14] Chadt A, Al-Hasani H. Glucose transporters in adipose tissue, liver, and skeletal muscle in metabolic health and disease. *Pflugers Arch* 2020; 472(9): 1273-98. [http://dx.doi.org/10.1007/s00424-020-02417-x] [PMID: 32591906]
- [15] Bryant NJ, Gould GW. Insulin stimulated GLUT4 translocation – Size is not everything! *Curr Opin Cell Biol* 2020; 65: 28-34. [http://dx.doi.org/10.1016/j.ceb.2020.02.006] [PMID: 32182545]
- [16] Li M, Chi X, Wang Y, Setrerrahmane S, Xie W, Xu H. Trends in insulin resistance: Insights into mechanisms and therapeutic strategy. *Signal Transduct Target Ther* 2022; 7(1): 216. [http://dx.doi.org/10.1038/s41392-022-01073-0] [PMID: 35794109]
- [17] Lee S, Rauch J, Kolch W. Targeting MAPK signaling in cancer: Mechanisms of drug resistance and sensitivity. *Int J Mol Sci* 2020; 21(3): 1102. [http://dx.doi.org/10.3390/ijms21031102] [PMID: 32046099]
- [18] Leto D, Saltiel AR. Regulation of glucose transport by insulin: Traffic control of GLUT4. *Nat Rev Mol Cell Biol* 2012; 13(6): 383-96. [http://dx.doi.org/10.1038/nrm3351] [PMID: 22617471]
- [19] Posner BI. Insulin signalling: The inside story. *Can J Diabetes* 2017; 41(1): 108-13. [http://dx.doi.org/10.1016/j.cjcd.2016.07.002] [PMID: 27614806]
- [20] Choi E, Bai XC. The activation mechanism of the insulin receptor: A structural perspective. *Annu Rev Biochem* 2023; 92(1): 247-72. [http://dx.doi.org/10.1146/annurev-biochem-052521-033250] [PMID: 37001136]
- [21] Ahmed Z, Pillay TS. Adapter protein with a pleckstrin homology (PH) and an Src homology 2 (SH2) domain (APS) and SH2-B enhance insulin-receptor autophosphorylation, extracellular-signal-regulated kinase and phosphoinositide 3-kinase-dependent signalling. *Biochem J* 2003; 371(2): 405-12. [http://dx.doi.org/10.1042/bj20021589] [PMID: 12521378]
- [22] Storz P, Toker A. 3'-phosphoinositide-dependent kinase-1 (PDK-1) in PI 3-kinase signaling. *Front Biosci* 2002; 7(1-3): d886-902. [http://dx.doi.org/10.2741/storz] [PMID: 11897568]
- [23] Vara JÁF, Casado E, de Castro J, Cejas P, Belda-Iniesta C, González-Barón M. PI3K/Akt signalling pathway and cancer. *Cancer Treat Rev* 2004; 30(2): 193-204. [http://dx.doi.org/10.1016/j.ctrv.2003.07.007] [PMID: 15023437]
- [24] Song G, Ouyang G, Bao S. The activation of Akt/PKB signaling pathway and cell survival. *J Cell Mol Med* 2005; 9(1): 59-71. [http://dx.doi.org/10.1111/j.1582-4934.2005.tb00337.x] [PMID: 15784165]
- [25] Janecka-Widła A, Majchrzyk K, Mucha-Malecka A, Slonina D, Biesaga B. Prognostic potential of Akt, pAkt(Ser473) and pAkt(Thr308) immunoreactivity in relation to HPV prevalence in head and neck squamous cell carcinoma patients. *Pathol Res Pract* 2022; 229: 153684. [http://dx.doi.org/10.1016/j.prp.2021.153684] [PMID: 34839095]
- [26] Shanak S, Bassalat N, Barghash A, Kadan S, Ardah M, Zaid H. Drug discovery of plausible lead natural compounds that target the insulin signaling pathway: Bioinformatics approaches. *Evid Based Complement Alternat Med* 2022; 2022: 1-42. [http://dx.doi.org/10.1155/2022/2832889] [PMID: 35356248]
- [27] Liang J, Oyang L, Rao S, et al. Rac1, a potential target for tumor therapy. *Front Oncol* 2021; 11: 674426. [http://dx.doi.org/10.3389/fonc.2021.674426] [PMID: 34079763]
- [28] Chiu TT, Jensen TE, Sylow L, Richter EA, Klip A. Rac1 signalling towards GLUT4/glucose uptake in skeletal muscle. *Cell Signal* 2011; 23(10): 1546-54. [http://dx.doi.org/10.1016/j.cellsig.2011.05.022] [PMID: 21683139]
- [29] Hopkins BD, Goncalves MD, Cantley LC. Insulin-PI3K signalling: An evolutionarily insulated metabolic driver of cancer. *Nat Rev Endocrinol* 2020; 16(5): 276-83. [http://dx.doi.org/10.1038/s41574-020-0329-9] [PMID: 32127696]
- [30] Blahova J, Martiniakova M, Babikova M, Kovacova V, Mondockova V, Omelka R. Pharmaceutical drugs and natural therapeutic products for the treatment of type 2 diabetes mellitus. *Pharmaceuticals* 2021; 14(8): 806. [http://dx.doi.org/10.3390/ph14080806] [PMID: 34451903]

- [31] Uusitupa M, Khan TA, Vigiulouk E, *et al.* Prevention of type 2 diabetes by lifestyle changes: A systematic review and meta-analysis. *Nutrients* 2019; 11(11): 2611. [http://dx.doi.org/10.3390/nu1112611] [PMID: 31683759]
- [32] Chaudhury A, Duvoor C, Reddy Dendi VS, *et al.* Clinical review of antidiabetic drugs: Implications for type 2 diabetes mellitus management. *Front Endocrinol* 2017; 8: 6. [http://dx.doi.org/10.3389/fendo.2017.00006] [PMID: 28167928]
- [33] Vithian K, Hurel S. Microvascular complications: Pathophysiology and management. *Clin Med* 2010; 10(5): 505-9. [http://dx.doi.org/10.7861/clinmedicine.10-5-505] [PMID: 21117389]
- [34] Huang D, Refaat M, Mohammedi K, Jayyousi A, Al Suwaidi J, Abi Khalil C. Macrovascular complications in patients with diabetes and prediabetes. *BioMed Res Int* 2017; 2017: 1-9. [http://dx.doi.org/10.1155/2017/7839101] [PMID: 29238721]
- [35] Blicklé JF, Andres E, Neyrolles N, Brogard JM. [Present status in the treatment of type 2 diabetes mellitus. Insulin-secreting agents]. *Rev Med Interne* 1999; 20(Suppl. 3): 351s-9s. [http://dx.doi.org/10.1016/S0248-8663(99)80508-6] [PMID: 10480186]
- [36] Altaf QA, Barnett AH, Tahrani AA. Novel therapeutics for type 2 diabetes: Insulin resistance. *Diabetes Obes Metab* 2015; 17(4): 319-34. [http://dx.doi.org/10.1111/dom.12400] [PMID: 25308775]
- [37] Di Magno L, Di Pastena F, Bordon R, Coni S, Canettieri G. The mechanism of action of biguanides: New answers to a complex question. *Cancers* 2022; 14(13): 3220. [http://dx.doi.org/10.3390/cancers14133220] [PMID: 35804992]
- [38] Chen Y, Ma H, Zhu D, *et al.* Discovery of novel insulin sensitizers: Promising approaches and targets. *PPAR Res* 2017; 2017: 1-13. [http://dx.doi.org/10.1155/2017/8360919] [PMID: 28659972]
- [39] Artasensi A, Pedretti A, Vistoli G, Fumagalli L. Type 2 diabetes mellitus: A review of multi-target drugs. *Molecules* 2020; 25(8): 1987. [http://dx.doi.org/10.3390/molecules25081987] [PMID: 32340373]
- [40] Lau ANC, Tang T, Halapy H, Thorpe K, Yu CHY. Initiating insulin in patients with type 2 diabetes. *CMAJ* 2012; 184(7): 767-76. [http://dx.doi.org/10.1503/cmaj.110779] [PMID: 22470171]
- [41] Abu-Lafi S, Rayan B, Kadan S, Abu-Lafi M, Rayan A. Anticancer activity and phytochemical composition of wild *Gundelia tournefortii*. *Oncol Lett* 2018; 17(1): 713-7. [http://dx.doi.org/10.3892/ol.2018.9602] [PMID: 30655821]
- [42] Hani N, Abulaila K, Howes MJR, *et al.* *Gundelia tournefortii* L. (Akkoub): A review of a valuable wild vegetable from Eastern Mediterranean. *Genet Resour Crop Evol* 2024. in press [http://dx.doi.org/10.1007/s10722-024-01927-2]
- [43] Dharsono HDA, Putri SA, Kurnia D, Dudi D, Satari MH. *Ocimum* species: A review on chemical constituents and antibacterial activity. *Molecules* 2022; 27(19): 6350. [http://dx.doi.org/10.3390/molecules27196350] [PMID: 36234883]
- [44] Azizah NS, Irawan B, Kusmoro J, *et al.* Sweet basil (*Ocimum basilicum* L.)—A review of its botany, phytochemistry, pharmacological activities, and biotechnological development. *Plants* 2023; 12(24): 4148. [http://dx.doi.org/10.3390/plants12244148] [PMID: 38140476]
- [45] Kadan S, Sasson Y, Saad B, Zaid H. *Gundelia tournefortii* antidiabetic efficacy: Chemical composition and GLUT4 translocation. *Evid Based Complement Alternat Med* 2018; 2018: 1-8. [http://dx.doi.org/10.1155/2018/8294320] [PMID: 29853973]
- [46] Guardado Yordi E, Matos MJ, Buso P, *et al.* A comprehensive ethnobotanical profile of *Ocimum campechianum* (Lamiaceae): From traditional medicine to phytochemical and pharmacological evidences. *Plant Biosyst* 2022; 156(6): 1388-404. [http://dx.doi.org/10.1080/11263504.2022.2056647]
- [47] Magar RA, Mallik AR, Chaudhary S, Parajuli S. Ethno-medicinal plants used by the people of Dharan, Eastern Nepal. *Indian J Tradit Knowl* 2022; 21(1): 72-80.
- [48] Dhama K, Sharun K, Gugjoo MB, *et al.* A comprehensive review on chemical profile and pharmacological activities of *Ocimum basilicum*. *Food Rev Int* 2023; 39(1): 119-47. [http://dx.doi.org/10.1080/87559129.2021.1900230]
- [49] Bottegoni G. Protein-ligand docking. *Front Biosci* 2011; 16(1): 2289-306. [http://dx.doi.org/10.2741/3854] [PMID: 21622177]
- [50] Bhatarai B, Walters WP, Hop CECA, Lanza G, Ekens S. Opportunities and challenges using artificial intelligence in ADME/Tox. *Nat Mater* 2019; 18(5): 418-22. [http://dx.doi.org/10.1038/s41563-019-0332-5] [PMID: 31000801]
- [51] Daina A, Michielin O, Zoete V. SwissADME: A free web tool to evaluate pharmacokinetics, drug-likeness and medicinal chemistry friendliness of small molecules. *Sci Rep* 2017; 7(1): 42717. [http://dx.doi.org/10.1038/srep42717] [PMID: 28256516]
- [52] Domínguez-Villa FX, Durán-Iturbide NA, Ávila-Zárraga JG. Synthesis, molecular docking, and *in silico* ADME/Tox profiling studies of new 1-aryl-5-(3-azidopropyl)indol-4-ones: Potential inhibitors of SARS CoV-2 main protease. *Bioorg Chem* 2021; 106: 104497. [http://dx.doi.org/10.1016/j.bioorg.2020.104497] [PMID: 33261847]
- [53] Kadan S, Saad B, Sasson Y, Zaid H. *In vitro* evaluation of anti-diabetic activity and cytotoxicity of chemically analysed *Ocimum basilicum* extracts. *Food Chem* 2016; 196: 1066-74. [http://dx.doi.org/10.1016/j.foodchem.2015.10.044] [PMID: 26593590]
- [54] Kadan S, Melamed S, Benvalid S, Tietel Z, Sasson Y, Zaid H. *Gundelia tournefortii*: Fractionation, chemical composition and GLUT4 translocation enhancement in muscle cell line. *Molecules* 2021; 26(13): 3785. [http://dx.doi.org/10.3390/molecules26133785] [PMID: 34206320]
- [55] Kim S, Thiessen PA, Bolton EE, *et al.* PubChem substance and compound databases. *Nucleic Acids Res* 2016; 44(D1): D1202-13. [http://dx.doi.org/10.1093/nar/gkv951] [PMID: 26400175]
- [56] Lowe DM, Corbett PT, Murray-Rust P, Glen RC. Chemical name to structure: OPSIN, an open source solution. *J Chem Inf Model* 2011; 51(3): 739-53. [http://dx.doi.org/10.1021/ci100384d] [PMID: 21384929]
- [57] O'Boyle NM, Banck M, James CA, Morley C, Vandermeersch T, Hutchison GR. Open babel: An open chemical toolbox. *J Cheminform* 2011; 3(1): 33. [http://dx.doi.org/10.1186/1758-2946-3-33] [PMID: 21982300]
- [58] Rizvi SMD, Shakil S, Haneef M. A simple click by click protocol to perform docking: AutoDock 4.2 made easy for non-bioinformaticians. *EXCLI J* 2013; 12: 831-57. [PMID: 26648810]
- [59] Borsari C, Keles E, Rageot D, *et al.* 4-(Difluoromethyl)-5-(4-((3 R, 5 S)-3,5-dimethylmorpholino)-6-(( R )-3-methylmorpholino)-1,3,5-triazin-2-yl)pyridin-2-amine (PQR626), a potent, orally available, and brain-penetrant mtor inhibitor for the treatment of neurological disorders. *J Med Chem* 2020; 63(22): 13595-617. [http://dx.doi.org/10.1021/acs.jmedchem.0c00620] [PMID: 33166139]
- [60] Garcia-Viloca M, Bayascas JR, Lluch JM, González-Lafont Á. Molecular insights into the regulation of 3-phosphoinositide-dependent protein kinase 1: Modeling the interaction between the kinase and the pleckstrin homology domains. *ACS Omega* 2022; 7(29): 25186-99. [http://dx.doi.org/10.1021/acsomega.2c02020] [PMID: 35910176]
- [61] Du-Cuny L, Song Z, Moses S, *et al.* Computational modeling of novel inhibitors targeting the Akt pleckstrin homology domain. *Bioorg Med Chem* 2009; 17(19): 6983-92. [http://dx.doi.org/10.1016/j.bmc.2009.08.022] [PMID: 19734051]
- [62] Sriramulu DK, Lee SG. Effect of molecular properties of the protein-ligand complex on the prediction accuracy of AutoDock. *J Mol Graph Model* 2021; 106: 107921. [http://dx.doi.org/10.1016/j.jmgm.2021.107921] [PMID: 33887523]
- [63] Meng XY, Zhang HX, Mezei M, Cui M. Molecular docking: A powerful approach for structure-based drug discovery. *Curr Computeraided Drug Des* 2011; 7(2): 146-57. [http://dx.doi.org/10.2174/157340911795677602] [PMID: 21534921]
- [64] Forli S, Huey R, Pique ME, Sanner MF, Goodsell DS, Olson AJ. Computational protein-ligand docking and virtual drug screening with the AutoDock suite. *Nat Protoc* 2016; 11(5): 905-19. [http://dx.doi.org/10.1038/nprot.2016.051] [PMID: 27077332]
- [65] Lam WWT, Siu SWI. PyMOL mControl: Manipulating molecular visualization with mobile devices. *Biochem Mol Biol Educ* 2017; 45(1): 76-83. [http://dx.doi.org/10.1002/bmb.20987] [PMID: 27292587]
- [66] Morris GM, Goodsell DS, Huey R, Olson AJ. Distributed automated docking of flexible ligands to proteins: Parallel applications of AutoDock 2.4. *J Comput Aided Mol Des* 1996; 10(4): 293-304. [http://dx.doi.org/10.1007/BF00124499] [PMID: 8877701]
- [67] Seeliger D, de Groot BL. Ligand docking and binding site analysis with PyMOL and Autodock/Vina. *J Comput Aided Mol Des* 2010; 24(5): 417-22. [http://dx.doi.org/10.1007/s10822-010-9352-6] [PMID: 20401516]
- [68] Waring MJ. Lipophilicity in drug discovery. *Expert Opin Drug Discov* 2010; 5(3): 235-48. [http://dx.doi.org/10.1517/17460441003605098] [PMID: 22823020]
- [69] Leucuta SE. Selecting oral bioavailability enhancing formulations

- during drug discovery and development. *Expert Opin Drug Discov* 2014; 9(2): 139-50.  
[http://dx.doi.org/10.1517/17460441.2014.877881] [PMID: 24387781]
- [70] Wilkinson GR. Drug metabolism and variability among patients in drug response. *N Engl J Med* 2005; 352(21): 2211-21.  
[http://dx.doi.org/10.1056/NEJMr032424] [PMID: 15917386]
- [71] Zaid H, Tamrakar AK, Razzaque MS, Efferth T. Diabetes and metabolism disorders medicinal plants: A glance at the past and a look to the future 2018. *Evid Based Complement Alternat Med* 2018; 2018: 1-3.  
[http://dx.doi.org/10.1155/2018/5843298] [PMID: 30364074]
- [72] Chiappelli F, Prolo P, Cajulis OS. Evidence-based research in complementary and alternative medicine I: history. *Evid Based Complement Alternat Med* 2005; 2(4): 453-8.  
[http://dx.doi.org/10.1093/ecam/neh106] [PMID: 16322801]
- [73] He JH, Chen LX, Li H. Progress in the discovery of naturally occurring anti-diabetic drugs and in the identification of their molecular targets. *Fitoterapia* 2019; 134: 270-89.  
[http://dx.doi.org/10.1016/j.fitote.2019.02.033] [PMID: 30840917]
- [74] Shanak S, Bassalat N, Albzoor R, Kadan S, Zaid H. *In vitro* and *in silico* evaluation for the inhibitory action of *O. basilicum* methanol extract on  $\alpha$ -glucosidase and  $\alpha$ -amylase. *Evid Based Complement Alternat Med* 2021; 2021: 1-9.  
[http://dx.doi.org/10.1155/2021/5515775] [PMID: 34306136]
- [75] Carnagarin R, Dharmarajan AM, Dass CR. Molecular aspects of glucose homeostasis in skeletal muscle – A focus on the molecular mechanisms of insulin resistance. *Mol Cell Endocrinol* 2015; 417(C): 52-62.  
[http://dx.doi.org/10.1016/j.mce.2015.09.004] [PMID: 26362689]

© 2024 The Author(s). Published by Bentham Science Publisher.



This is an open access article distributed under the terms of the Creative Commons Attribution 4.0 International Public License (CC-BY 4.0), a copy of which is available at: <https://creativecommons.org/licenses/by/4.0/legalcode>. This license permits unrestricted use, distribution, and reproduction in any medium, provided the original author and source are credited.

**DISCLAIMER:** The above article has been published, as is, ahead-of-print, to provide early visibility but is not the final version. Major publication processes like copyediting, proofing, typesetting and further review are still to be done and may lead to changes in the final published version, if it is eventually published. All legal disclaimers that apply to the final published article also apply to this ahead-of-print version.